INVESTIGATION OF SURFACE PROPERTIES AND FeB-Fe$_2$B LAYER FORMATION IN PACK BORONIZING OF CEMENTATION STEEL

TANJU TEKER* and MURAT SARI

Department of Manufacturing Engineering,
Faculty of Technology, Sivas Cumhuriyet University,
58140 Sivas, Turkey
*tanjuteker@cumhuriyet.edu.tr

In this study, cementation steel was boronized at 1050°C for 6 h, 8 h, and 10 h. Microstructural change on the surface of the samples after boronization was detected by optical microscope (OM), scanning electron microscope (SEM), energy dispersive spectroscopy (EDS), X-Ray diffraction (XRD), and electron back scatter diffraction (EBSD) analyses. Also, surface roughness, microhardness, and layer thickness were measured. FeB, Fe$_2$B phases, and saw tooth morphology expected in iron-based metals during boring process occurred in the entire process time. The average layer thickness of the boronized samples at 1050°C for 10 h was measured as 222 μm and the surface roughness value was 3.40 μm. The hardness of boride phases acquired on the samples varied between 1700 HV and 1730 HV. As a result, while the ratio of chromium carbide is the highest in the base metal, the boron level was the highest in the coating. Compounds 49 wt.% Cr$_7$C$_3$ and 47 wt.% B were identified as the most intensely concentrated.

Keywords: Boronizing; cementation steel; surface roughness; layer thickness.

1. Introduction

Boron method, which is accepted as one of the surface modification processes, provides to serve for a longer period of time by improving the properties of the materials in the service area. The advantages of boronozing increase the high oxidation resistance, hardness, wear, and corrosion resistance of the surface of metals and alloys. Boron is generally used for alloying or surface hardening of iron-based materials. The mechanism of boronization is the spreading of boron atoms to the metal surface by the effect of heat energy and form suitable borides with the main metal atoms.[1–4] The physical state of the boron

source may be solid, liquid, or gas. Boronizing is generally carried out at a temperature range of 800–1100°C for 1–12 h. The filler material and deoxidants retain oxygen during boronizing to form a reducing atmosphere. The methods used during the boring process, material composition, material type, processing time, and temperature are the factors that affect the layer obtained. At high temperatures, boron is emitted to the surface of the steel material and boride layers containing Fe$_2$B and/or FeB phases are obtained.[5–7] The hardness and abrasion resistance of the steels can be increased significantly with the layers obtained by boron diffusion. Boronizing can be

---

*Corresponding author.

applied to both ferroalloys produced by powder and other methods.

Boronization can be applied to alloys with refractory metals such as Zr, Ta, Nb, Hf, Mo, and W. The greatest advantage of the layers formed as a result of boring is the high melting temperature and the extremely high hardness of the formed phases.[8,9] The hardness of the boron layers is higher than the hardness of hardened tool steels and hard chromium-coated metals but is equal to the hardness of tungsten carbide.[10,11] Boronizing of materials is obtained at lower cost and is better resistive to materials instead of costly workpieces. This process provides both financial advantage and solves parts and time problems by using boronized parts instead of original machine parts. In this way, it provides great benefits.[12] Yu *et al.*[13] reported boronozing by SPS pack-boriding on steel samples at 850°C with different treatment durations. Results demonstrated that the Fe_2B phase can be achieved by turning FeB to the Fe_2B phase due to the reduce in boron application in the boroning medium.

Filep and Farkas[14] fabricated a boride layer using plasma boriding. In the literature, the effects of package thickness of boronizing mixture, chemical content, and particle size of powder mixtures on the boron layer have been investigated.[15–17] Li *et al.*[18] investigated the effect of boronizing temperature and time on microstructure and abrasive performance of $Cr_{12}Mn_2V_2$. Bejar and Moreno[19] investigated the wear strength of boronized steels. Gopalakrishnan *et al.*[20] reported interrupted boronization of medium carbon steels. Cementation steels are low-carbon and unalloyed steels that are hard on the surface, resistant to wear, and softer and tougher in the core. It is used in the manufacture of gears, shafts, piston pins, cutting tools, and impact resistant parts. With boronizing, the surface properties, strength, and working conditions of the steel can be perfectibled.

In this study, the effect of processing time on surface properties and FeB-Fe_2B layer formation in pack boronizing of cementation steel at 1050°C process temperature for 6 h, 8 h, and 10 h treatment time was investigated experimentally. The study aims to fabricate the minimal surface thickness and to determine the phase intensities in boronized a cementation steel.

2. Materials and Method

The cementation steel chosen for the boronizing process has chemical contents (Bal. wt.%Fe, 0.74 wt. %Mn, 0.48 wt.%Cr, 0.20 wt.%C, 0.20 wt.%Mo, 0.020 wt.%P, 0.015 wt.%S, and 0.30 wt.%Si). Commercially available Ekabor II [5% B_4C (donor), 90% SiC (diluent), 5% KBF_4 (activator)] boron donor powder was used for boronizing. The properties of Ekabor II powder are given in Table 1. In order to reduce the moisture content of boron powders to minimum levels, it was subjected to 24 h drying at 100°C in a vacuum MMM-Group branded furnace. Samples were cut to the desired dimensions for boronizing. Then, the surfaces of the samples were sanded with 80–1200 mesh Emery paper. The samples were polished with 1–3 μm diamond paste to ensure the desired surface quality for boronizing. The samples were kept for 10 min in ethyl alcohol (ethanol C_2H_5OH) to remove residues from the sample surfaces. The samples were dried well and prepared for boriding. Boronizing was performed using a digitally controlled Protherm furnace. The sample to be boronized was placed in the silicon-carbide melting pot. The sample was buried in a 4–5 cm boron donor medium provided boron powder was on top and bottom (Fig. 1). On top of the boron powder, the SiC-based amorphous phase ecrite powder and alumina powder produced by Bortec company, which acts as deoxidant, were placed to preserve the material from oxidation. After the process was completed, the pot

Table 1. The properties of Ekabor II powder.

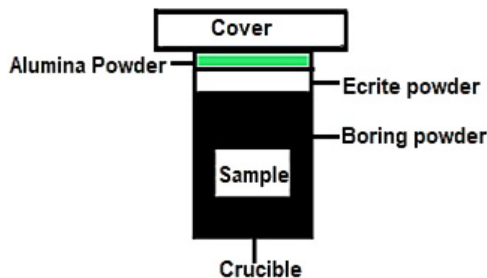| Powder type	Grain size	Intensity
Ekabor II	$\leq 850\,\mu$m	1.50

Fig. 1. (Color online) The array shape in the melting crucible of the sample.

cover was tightly closed and made ready for boronizing. Cementation steel was boronized at 1050°C for 6 h, 8 h, and 10 h.

Optical microscope (LEICA DM750) and scanning electron microscope (SEM) (ZEISS, EVO LS10) were employed to reveal the coating morphology and layer thicknesses of borides formed after boronizing. The phases and compounds were determined using BRUKER X-ray diffractometer RadB-DMAX II, Cu Kα radiation, $\lambda = 1.5418$ Å wavelength. The elementary composition was analyzed by energy dispersive spectrometer (EDS) and surface mapping methods. The hardness changes were carried out on a Vickers (HV) scale at 0.5 mm intervals with a QNESS Q10 microhardness device under a load of 30 g for 5 s. Phase distributions were analyzed by electron back scatter diffraction (EBSD) analysis. Surface roughness values were measured with MITUTOYO SJ-210 model device.

3. Results and Discussion

3.1. *Evaluation of macro- and micro-structures*

Macro-images of the test samples before and after boronizing are given in Figs. 2(a) and 2(b). The high boronizing process temperature had a remarkable influence on the coating surface quality of the sample. In boronizing, the diffusion of boron atoms into the lattice of a matrix alloy creates boronized composites. The penetration of boron atoms intensifies with temperature. The causes for using high temperature for boriding are: (a) thermally induced void creation in the matrix and (b) mobility of boron atoms to pass over the energy obstacle for diffusion. Boron diffuses fast at 1050°C, resulting in greater homogeneity with less cracking and gaps.[21,22] The single-phase boride layer consists of Fe_2B produced on boronized cementation steel for up to 6 h. Since FeB and Fe_2B

are fabricated under tensile and residual tensions, cracks usually appear at the interface of a double-phase layer.[23] Some porosities and agglomerates between FeB and Fe_2B phases were detected on the surface of samples boronized for 6 h and 8 h at 1050°C. Boride manufactured on the surface of the substrate had a dentritic morphology. The colonicity at the FeB/Fe_2B interface was lower than the Fe_2B/substrate interface, as demonstrated in Fig. 1. The high boronizing process temperature increased the roughness coefficient on the sample surfaces. When a proper boron intesity is attained at some places on the surface of the substrate, Fe_2B started to nucleate.

The optical and SEM micrographs of the boride layers on the surfaces of the boronized samples at 6 h, 8 h, and 10 h processing times are given in Figs. 3 and 4. Boride coating had two separate layers which were outer layer (dark) and the inner layer (white) as shown in Fig. 3. These show that the boron atoms in the borid layer were more intensived in the external layer of the borid covering than in the interior. As shown in Fig. 3, the thickness of the coating and transition zones of the test samples increased. The coating thickness (222 μm) in the boronized sample for 10 h was higher than the boronized sample for 8 h. The coating thickness (203 μm) in the boronized sample for 8 h was higher than the the coating thickness (172 μm) of boronized sample for 6 h. The layer thicknesses that emerged at 1050°C and 10 h were the highest. The processing time affected the size of the layer thickness. Diffusion deep and the size of the boride layer increased during boronozing due to high temperature and time. As boron atoms diffuse into the matrix of the boride layer, boron diffusion is hard and the boron rate on the surface rises. This causes the appearance of the FeB. This coating method can be defined as follows: (1) the cementation steel having high carbon content. Due to the fact that the carbon element cannot fully dissolve in iron
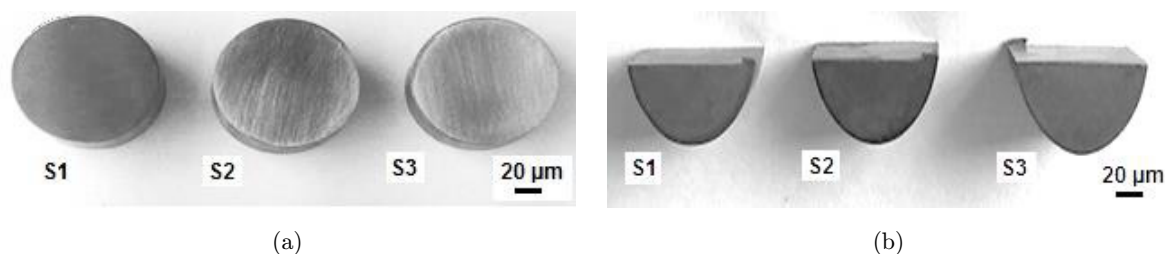

(a)   (b)

Fig. 2.   Macro-images of the test samples (a) before boronizing and (b) after boronozing.
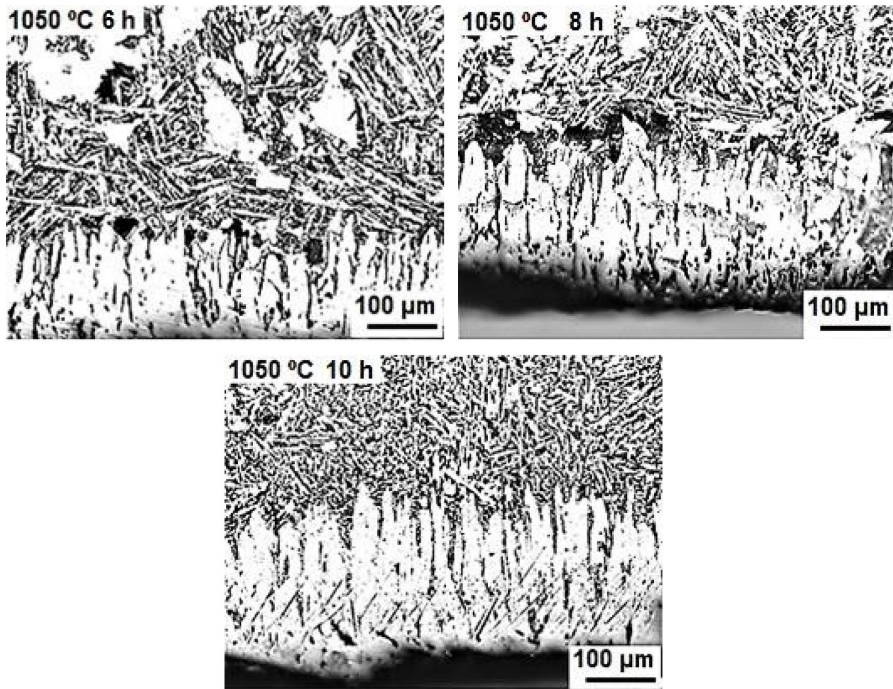
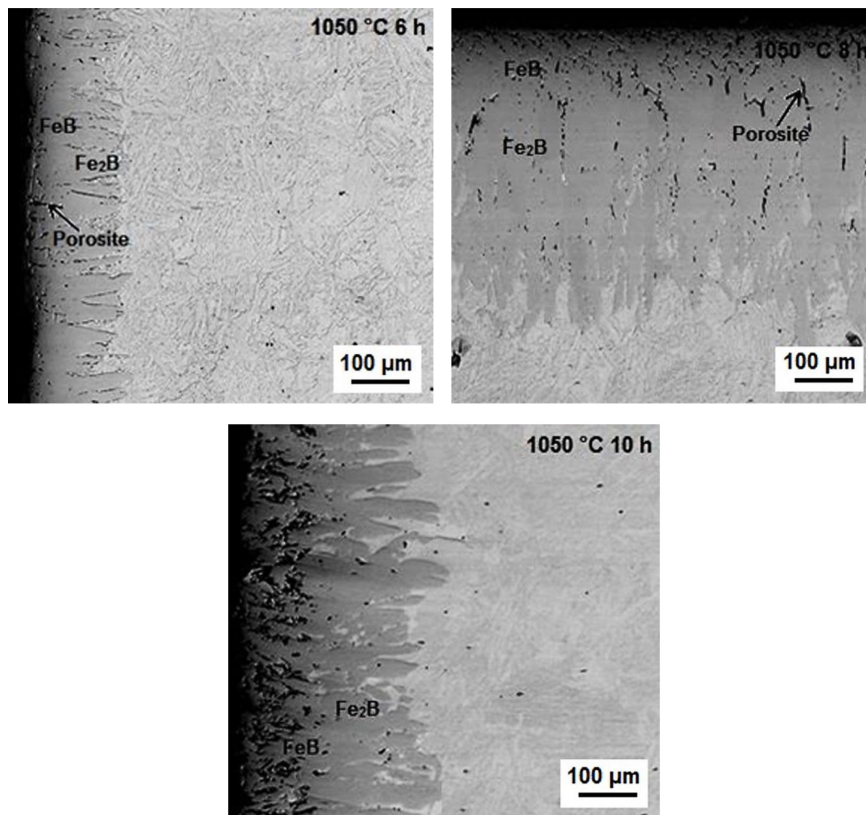Fig. 3.   Optical images of the boronized samples at 1050°C.

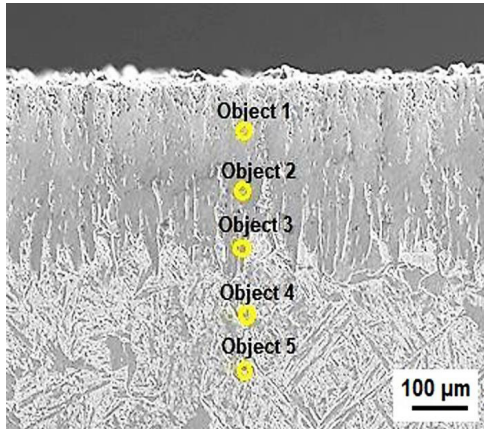Fig. 4.   SEM micrographs of the boronized samples at 1050°C.

Fig. 5. (Color online) SEM micrographs showing EDS analysis points of boronized sample at 10 h.

boride structure, carbon content can be denser beneath the iron boride layer while carbon element diffuses into the substrate material. Therefore, the boride layers cannot easily diffuse and the boride layer formation was blocked. (2) The V and Cr content in the cementation steel plays a negative role in the iron boron diffusivity.[23,24] This was because these elements could enter to the lattice of iron boride. Consequently, the thickness of boride layer would decline. The thickness of coated layer is affected by alloying elements such as carbon, vanadium, and chrome, which means that the diffusivity of boron layer can be changed negatively. In addition, the reactivity between metal and boron could be altered by the modifications that occurred in the composition and surface of the metal substrate, as a result of redistribution of alloying element after boron treatment.

EDS analysis of boronized samples for 10 h is shown in Figs. 5 and 6. Boring time, temperature, boronizing powder composition, and chemical content change boron diffusion.[25] As understood from Figs. 5 and 6, the maximum boron concentration was observed in sample treated with boron for 10 h. This is because process tempreture and process time were at high levels. This situation means that diffusion was high. EDS analysis indicated that concentration of iron in the boride layer was lower rather than the substrate material. In addition, Cr, Ni, Mo, V, and W elements alloyed in iron matrix was dissolved in the borided layers of samples. However, these alloying elements in iron matrix prevented the concentration of the boron layers into substrate material. This is because these alloying elements did not dissolve in the
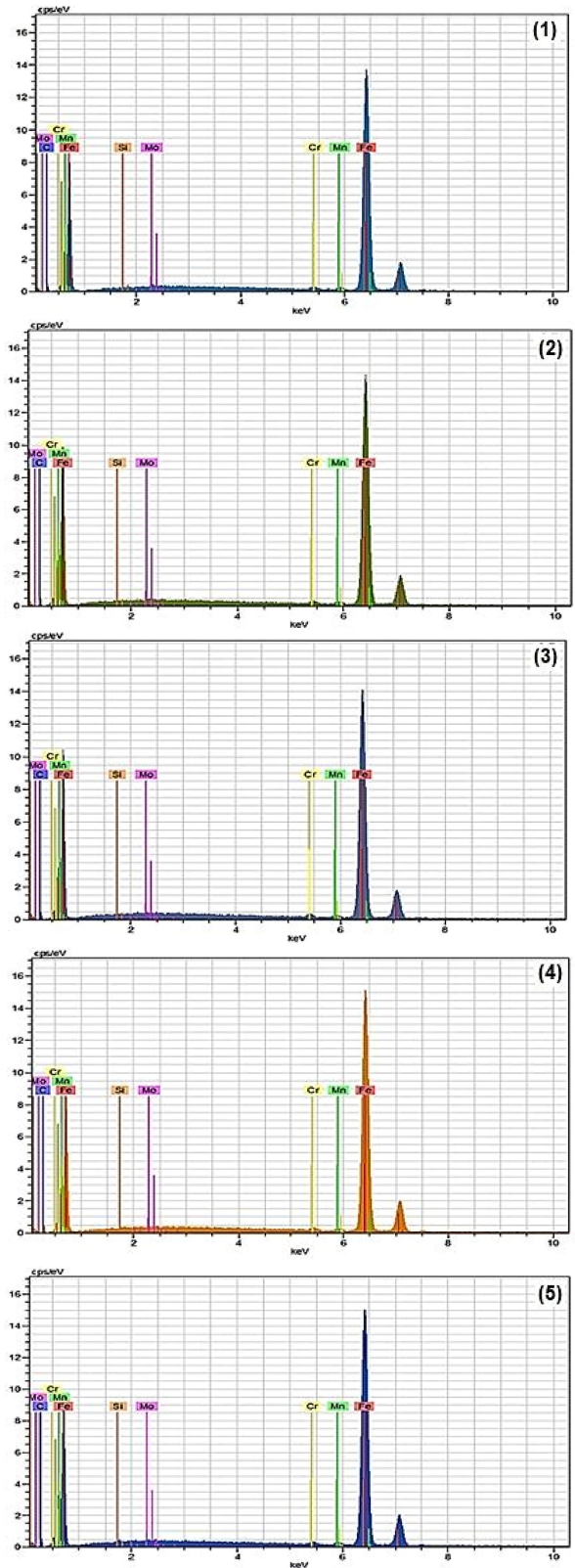

Fig. 6. (Color online) EDS analysis graphs of boronized sample for 10 h.

boride layer. Also, they blocked the growth of boride layers into matrix. The boron ratio in the boride layer was higher than the B ratio in the transition zone. The Fe ratio in the boride layer was lower than in the transition zone. C and Si did not dissolve in the boride layer and were repulsed from the surface by boron atoms.

3.2. *Microhardness*

The microhardness-distance curves of boronized samples at 6 h, 8 h, and 10 h are displayed in Fig. 7. Borides (FeB and Fe_2B), transition zone, and matrix exhibited unlike hardness. Boriding at higher temperatures fabricated a harder FeB and rised hardness. The porosity in the boride layer declined the hardness. The boron layer was harder than the matrix. The hardness of the base metal of the boronized sample during the 6 h process was 160 HV, while this value was 1700 HV in the boride layer. In case of cementation steel boronized in 8 h, the hardness of the base metal was 165 HV, whereas it was 1730 HV in the boride layer. In case of cementation steel boronized in 10 h, the hardness value of the base metal was 165 HV, while it was approximately 1720 HV in the boride layer. The hardness of the FeB layer on the surface of the boride coating was harder than the Fe_2B layer. Temperature and time provided the driving force required for the diffusion.[25,26] In addition, it was found that there were differences between the hardness values of vickers traces taken from the same distances in the boride layer of the same samples. There are two reasons for these
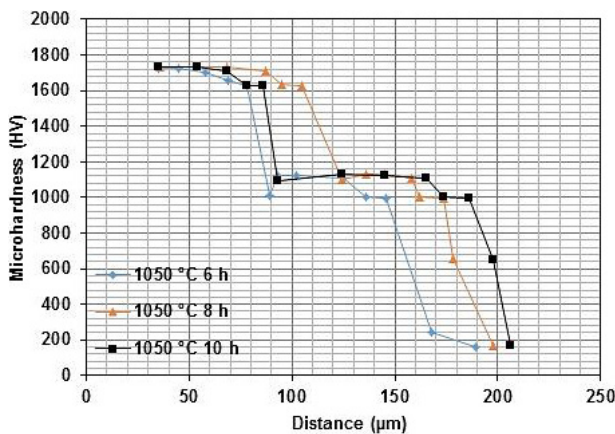

Fig. 7. (Color online) The microhardness-distance curves of cementation steel boronized at $1050°C$ for 6 h, 8 h, and 10 h.

differences: The first is that each boride exhibits different elastic-plastic behavior. The second is the orientation differences and the porosity of the layer. Some studies indicated that thermal coefficient of boride layers was different from thermal coefficient of steel.[27,28] If this difference was too large, cracks would occur in transition zone between steel and boron layer. Same situation was also true for Fe_2B and FeB boron layers which were formed on the surface of substrate material. In terms of mechanical properties such as wear resistance and thermal resistance, Fe_2B and FeB formed on the surface of substrate material made it more resistant. The decrease in microhardness can attribute to concentration of the silicon atom in boron layer since silicon did not dissolve into matrix, which means that the microhardness decreased. In addition, as it went through to the depth substrate material, a decrease in hardness occurred because there was matrix whose microhardness was lower than boron layer. Therefore, microhardness decreased in the matrix structure. Accordingly, microhardness value of boride layer was recorded as about 1750 HV which was much more than matrix structure. Also, as understood from the literature, alloying elements played a crucial role on the microhardness of boron layers since the stoichiometric characteristic of the boron layer was different from matrix (steel).[29–31] The higher hardness of the transition zone just below the boride layer is due to the hardening of a solid solution between iron and B.

3.3. *XRD phase analysis*

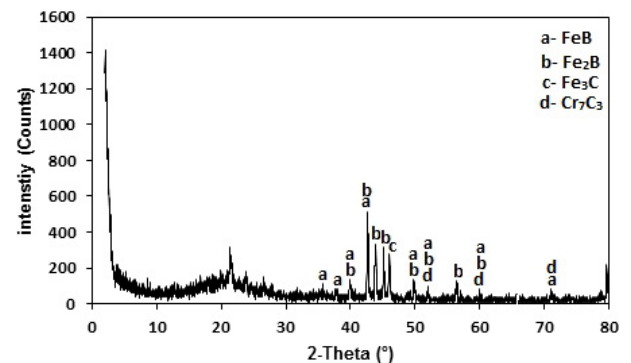XRD analysis pattern of cementation steel boronized at 10 h is indicated in Fig. 8. As a result of XRD

Fig. 8. X-ray diffraction analysis of cementation steel boronized at 10 h.

analysis, FeB and Fe$_2$B were found as the main phases. Cr$_7$C$_3$ and Fe$_3$C phases were also obtained. The reason for the formation of the Fe$_3$C phase was the penetration of XRD rays to the substrate of the coating due to the level and density of porosity that occurred during the coating with increasing process temperature and time. It was understood from the XRD pattern that although the surface of the samples was covered with the FeB phase, the most intense peak was observed in the Fe$_2$B phase. The reason for this is Fe$_2$B phase formed beneath the FeB phase was thicker than FeB phase. The inner part of the Fe$_2$B phase is formed from boride crystals which arranged with their crystallographic axis oriented perpendicularly to the surface of the sample.

3.4. *Surface roughness of coatings*

The surface roughness analysis results of cementation steel boronized at 6 h, 8 h, and 10 h are shown in Fig. 9. The surface roughness level of cementation steel boronized at 1050°C for 6 h was 1.20 μm and the surface roughness level of the sample boronized for 8 h was 1.90 μm. The surface roughness of the sample boronized for 10 h was 3.40 μm. The average value at 1050°C process temperature was measured as 2.15 μm. Surface roughness levels of samples boronized at different times grew up. Accordingly, maximum surface roughness value was recorded on sample boronized at 1050°C for 10 h. The faster reaction kinetic occurred on surface of this sample. Surface roughness is related to kinetic of chemical reaction that happened on the surface.[32,33]
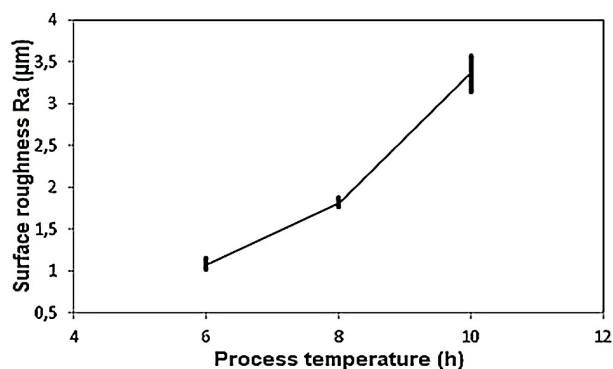

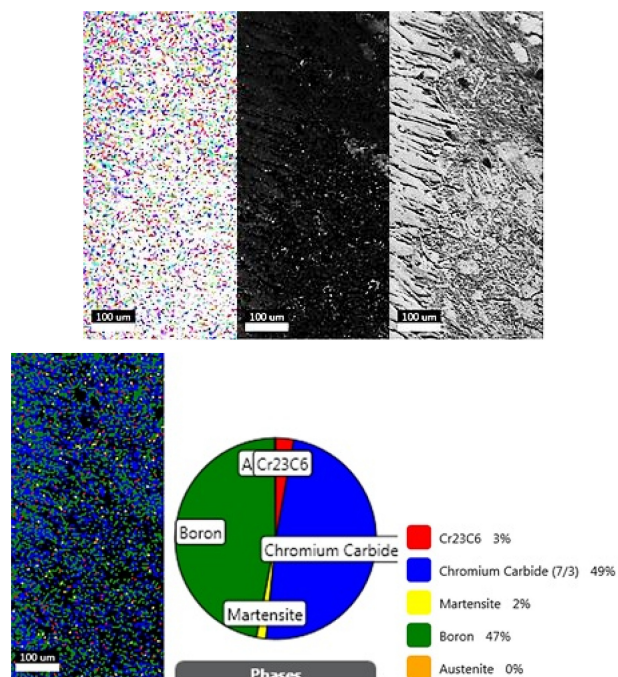Fig. 9. Surface roughness analysis results of boronized cementation steel at 6 h, 8 h, and 10 h.

Fig. 10. (Color online) EBSD analysis results of cementation steel boronized at 10 h.

3.5. *EBSD analysis*

EBSD analysis of the sample boronized for 10 h is represented in Fig. 10. It was noticed that the FeB was near the surface and Fe$_2$B was near the iron matrix. A longer boron time produced more FeB borides. As can be exhibited in Fig. 10, Cr$_7$C$_3$ compound was determined as the most intense compound (49 wt.%). During boron treatment, process temperature was above the A$_3$ temperature and samples were subject to supercooling, which means that it can lead to formation of chrome carbide compounds. On the boron layer, the most intense compound was boron element (47 wt.%). This situation showed that diffusion of boron occurred in the matrix structure.

4. Conclusions

In this study, the effect of processing time on the coating area formed after boronizing process for 6 h, 8 h, and 10 h at 1050°C was investigated experimentally. The following results were reached:

- Cementation steel was boronized by pack boronizing method. Saw tooth morphology occurred at all boring times.

- Fe$_2$B and FeB phases expected in ferrous metals were formed in the cementation steel.
- Due to the high temperature and time (1050°C for 10 h), the thickness level of the coating increased.
- Diffusion deep of boron and size of the boride layer increased during boronozing due to high temperature and the longer time.
- The boron concentration of the sample boronized at 1050°C for 10 h was greater.
- The surface roughness level of the samples boronized at 1050°C for 10 h was the highest.
- A significant rise in hardness values was observed. The surface hardness of the borided cementation steel was in the range of 1700–1730 HV, while the unborided steel substrate was 700–750 HV.
- Compounds 49 wt.% Cr$_7$C$_3$ and 47 wt.% B were identified as the most intensely concentrated.

Acknowledgment

References

1. I. Campos-Silva, M. Domínguez, N. Lopez-Perrusquia, A. Meneses-Amador, R. Escobar Galindo and J. Martınez-Trinidad, *Appl. Surf. Sci.* **256** (2010) 2372.
2. O. Yılmaz, T. Teker and S. Karataş, *Prot. Met. Phys. Chem. Surf.* **52** (2016) 119.
3. G. K. Kariofillis, G. E. Kiourtsidis and D. N. Tsipas, *Surf. Coat. Technol.* **201** (2006) 19.
4. P. Geoeuriot, R. Fillet, F. Thevenot, J. H. Driver and H. Bruyas, *Mater. Sci. Eng.* **55** (1982) 9.
5. J. Subrahmanyam and K. Gopinath, *Wear* **95** (1984) 287.
6. P. Goeuriot, F. Thevenot, J. H. Driver and T. Magnin, *Wear* **86** (1983) 1.
7. M. Carbucicchio, G. Palombarini and G. Sanbogna, *J. Mater. Sci.* **19** (1984) 4035.
8. W. Fichtl, *Mater. Des.* **2** (1981) 276.
9. V. Jain and G. Sundararajan, *Surf. Coat. Technol.* **149** (2001) 21.
10. V. I. Dybkov, W. Lengauer and K. Barmak, *J. Alloy. Compd.* **398** (2005) 113.
11. I. Campos, J. Oseguera, U. Figueroa, J. A. Garcıa, O. Bautista and G. Kelemeni, *Mater. Sci. Eng. A* **352** (2003) 261.
12. O. Allaoui, N. Bouaouadja and G. Saindernan, *Surf. Coat. Technol.* **201** (2006) 3475.
13. L. G. Yu, X. J. Chen, K. A. Khor and G. Sundararajan, *Acta Mater.* **53** (2005) 2361.
14. E. Filep and S. Farkas, *Surf. Coat. Technol.* **199** (2005) 1.
15. V. Jain and G. Sundararajan, *Surf. Coat. Technol.* **149** (2002) 21.
16. C. Martini, G. Palombarini and M. Carbucicchio, *J. Mater. Sci.* **39** (2004) 933.
17. C. Meriç, S. Sahin and S. S. Yilmaz, *Mater. Res. Bull.* **35** (2000) 2165.
18. C. Li, B. Shen, G. Li and C. Yang, *Surf. Coat. Technol.* **202** (2008) 5882.
19. M. A. Bejar and E. Moreno, *J. Mater. Process. Technol.* **173** (2006) 352.
20. P. Gopalakrishnan, S. S. Ramakrishnan, P. Shankar and M. Palaniappa, *Metall. Mater. Trans. A* **33** (2002) 1475.
21. S. Sen, I. Ozbek, U. Sen and C. Bindal, *Surf. Coat. Technol.* **135** (2001) 173.
22. I. Ozbek and C. Bindal, *Surf. Coat. Technol.* **154** (2002) 14.
23. M. Keddam and S. M. Chentouf, *Appl. Surf. Sci.* **252** (2005) 393.
24. I. Campos-Silva, M. Ortiz-Domínguez, O. Bravo-Bárcenas, M. A. Doñu-Ruiz, D. Bravo-Bárcenas, C. Tapia-Quintero and M. Y. Jiménez-Reyes, *Surf. Coat. Technol.* **205** (2010) 403.
25. M. Kulka and A. Pertek, *Appl. Surf. Sci.* **214** (2003) 278.
26. C. Martini, G. Palombarini, G. Poli and D. Prandstraller, *Wear* **256** (2004) 608.
27. C. Martini, G. Palombarini and M. J. Carbucicchio, *Mater. Sci.* **39** (2004) 933.
28. G. Rodríguez-Castro, I. Campos-Silva, J. Martínez-Trinidad, U. Figueroa-López, D. Meléndez-Morales and J. Vargas-Hernández, *Adv. Mater. Res.* **65** (2009) 63.
29. S. Taktak, *Mater. Des.* **28** (2007) 1836.
30. C. Bindal and A. H. Ucisik, *Surf. Coat. Technol.* **94**–**95** (1997) 561.
31. M. A. Bejar and E. Moreno ,*J. Mater. Process. Technol.* **173** (2006) 352.
32. P. Gopalakrishnan, S. S. Ramakrishnan, P. Shankar and M. Palaniappa, *Metall. Mater. Trans. A* **33** (2002) 1475.
33. X. Yan, Z. Q. Wei, X. L. Wen, Z. G. Wu, J. W. Xu, W. M. Liu and J. Tian, *Appl. Surf. Sci.* **195** (2002) 74.